Journal of Cerebral Blood Flow & Metabolism (2015) 35, 1852–1861

www.jcbfm.com

ORIGINAL ARTICLE

The effects of perturbed cerebral blood flow and cerebrovascular reactivity on structural MRI and behavioral readouts in mild traumatic brain injury

Justin A Long[1,6], Lora T Watts[1,2,3,6], Wei Li[1], Qiang Shen[1], Eric R Muir[1], Shiliang Huang[1], Robert C Boggs[1], Abhinav Suri[1] and Timothy Q Duong[1,3,4,5]

This study investigated the effects of perturbed cerebral blood flow (CBF) and cerebrovascular reactivity (CR) on relaxation time constant (T_2), apparent diffusion coefficient (ADC), fractional anisotropy (FA), and behavioral scores at 1 and 3 hours, 2, 7, and 14 days after traumatic brain injury (TBI) in rats. Open-skull TBI was induced over the left primary forelimb somatosensory cortex ($N = 8$ and 3 sham). We found the abnormal areas of CBF and CR on days 0 and 2 were larger than those of the T_2, ADC, and FA abnormalities. In the impact core, CBF was reduced on day 0, increased to 2.5 times of normal on day 2, and returned toward normal by day 14, whereas in the tissue surrounding the impact, hypoperfusion was observed on days 0 and 2. CR in the impact core was negative, most severe on day 2 but gradually returned toward normal. T_2, ADC, and FA abnormalities in the impact core were detected on day 0, peaked on day 2, and pseudonormalized by day 14. Lesion volumes peaked on day 2 and were temporally correlated with forelimb asymmetry and foot-fault scores. This study quantified the effects of perturbed CBF and CR on structural magnetic resonance imaging and behavioral readouts.

Journal of Cerebral Blood Flow & Metabolism (2015) **35,** 1852–1861; doi:10.1038/jcbfm.2015.143; published online 24 June 2015

Keywords: functional outcomes; hypercapnia; MRI: diffusion tensor imaging; TBI

INTRODUCTION

Traumatic brain injury (TBI) is a leading cause of death and disability.[1] The initial physical impact causes direct mechanical damage, and is followed by progressive secondary injuries such as brain swelling, perturbed cerebral blood flow (CBF), abnormal cerebrovascular reactivity (CR), metabolic dysfunction, blood–brain-barrier disruption, inflammation, oxidative stress, and excitotoxicity, among others.[1] Disruptions in CBF and CR could be the result of either direct mechanical injury to vessels or indirect reduction of local perfusion pressure by elevated intracranial pressure. Disruption of CBF and CR *per se* could lead to metabolic stress, vascular dysfunction, neuronal dysfunction, ischemia, and cell death.

Cerebral blood flow measurements in TBI have been reported using radiolabeled microspheres,[2] laser speckle imaging,[3] laser Doppler flowmetry,[4] dynamic susceptibility contrast magnetic resonance imaging (MRI),[5] susceptibility-weighted MRI,[6] and arterial spin labeling MRI[7] in different TBI models with different degrees of severity. Hypoperfusion and hyperperfusion after TBI have been found in some animal models. CR (i.e., CBF response to 5% CO_2 inhalation) however has not been widely studied in TBI. Moreover, the effects of CBF and CR disruptions in TBI on other MRI parameters and tissue fate have not been systematically investigated. With advances in modern noninvasive imaging techniques, CBF, and NC can be readily measured in a noninvasive and longitudinal manner. The ability to image CBF and NC dysfunction have the potential to provide early and valuable information on TBI, and predict tissue fate and functional outcomes.

The goal of this study was to investigate spatiotemporal dynamics of CBF and CR in an established TBI model in rats and to determine how these hemodynamic disruptions affect T_2, ADC, FA, and lesion volume. An open-skull impact was applied over the left primary forelimb somatosensory cortex (S1FL) using the controlled cortical impact (CCI) device. Multimodal MRI measurements were made longitudinally from 1 to 3 hours, 2, 7, and 14 days post TBI. Comparisons were also made with behavioral assessments using foot-fault and forelimb asymmetry tests.

MATERIALS AND METHODS

ARRIVE Guidelines

The following ARRIVE guidelines were followed in the preparation of this manuscript: Title, Abstract, Background, Objectives, and Ethical statement; Study Design; Experimental procedures; Experimental animals, Housing and husbandry; Experimental outcomes; Statistical methods, Numbers

[1]Research Imaging Institute, University of Texas Health Science Center, San Antonio, Texas, USA; [2]Departments of Cellular and Structure Biology, University of Texas Health Science Center, San Antonio, Texas, USA; [3]Department of Neurology, University of Texas Health Science Center, Houston, Texas, USA; [4]Department of Opthalmology, University of Texas Health Science Center, San Antonio, Texas, USA and [5]South Texas Veterans Health Care System, San Antonio, Texas, USA. Correspondence: Dr TQ Duong, Research Imaging Institute, University of Texas Health Science Center at San Antonio, 8403 Floyd Curl Dr, San Antonio, Texas 78229, USA.
E-mail: duongt@uthscsa.edu
[6]These authors contributed equally to this work.
This work was supported in part by NIH/NINDS R01 NS45879 (TQD), a TL1 (JAL) and KL2 TR001118 and Mike Hogg Fund (LTW) via the Clinical Translational Science Awards (CTSA, parent grants UL1TR000149, TL1TR001119, and KL2TR001118).
Received 17 November 2014; revised 11 May 2015; accepted 22 May 2015; published online 24 June 2015

analyzed; Interpretation, and scientific implications; and Generalizability/translation and Funding.

Animal Preparations

Animal procedures followed guidelines and regulations consistent with the Guide for the Care and Use of Laboratory Animals, Public Health Service Policy on Humane Care and Use of Laboratory Animals, and the Animal Welfare Act and Animal Welfare Regulations and were approved by the Institutional Animal Care and Use Committee of the University of Texas Health Science Center San Antonio (protocol no. 13034). Experimental TBI was done as previously described.[8] Briefly, male Sprague Dawley rats (250–350 g, 3–6 months of age, $n=3$ sham-operated, $n=8$ CCI; Charles River Laboratories, O'Fallon, MO, USA) housed two to a cage in a Tecniplast caging system with autoclaved sani chip bedding. The rats had *ad libitum* access to irradiated rodent chow from Harlan laboratories and autoclaved water. The rats were anesthetized initially with 5% isoflurane mixed with room air and maintained at 1.5–2.0% isoflurane during surgery and 1.2% during imaging procedures. The animal was secured in a stereotaxic frame and a surgical incision was made posterior from the impact site (at the level of the cerebellum) to prevent artifacts during MRI acquisition and the periosteum was removed over the impact site. A 0.5 mm craniotomy was created over the left forelimb primary somatosensory cortex (S1FL: +0.25 mm anterior and 3.5 mm lateral to bregma), exposing the dura matter. The intact dura matter was impacted using a pneumatic controlled cortical impactor (Precision Systems and Instrumentation, LLC, Fairfax Station, VA, USA) fitted with a 0.3 mm tip (5.0 m/s, 250 μs dwell time, 1mm depth) to mimic a mild focal TBI. After the impact, the cranial opening was sealed with bone wax, the scalp sutured closed, and antibiotic ointment applied. Saline was injected under the skin to facilitate the removal of air pockets between the scalp and the skull to minimize artifacts during MRI acquisition. Buprenex (0.05 mg/kg) was given subcutaneously every 12 hours for 3 days for pain.

Magnetic resonance imaging was acquired at 1 and 3 hours post TBI and on 2, 7, and 14 days after TBI. Behavioral assessments were made 1 day before TBI and again 2, 7, and 14 days after TBI before the MRI experiments in the same animals. Behavioral tests were not performed on the day of TBI induction because of incomplete recovery from anesthesia. Immunohistology was done after MRI 14 days post TBI. The 14-day end point was selected based on a subset of studies in which no apparent difference in lesion volumes between 14 and 28 days post TBI were observed.

Blood pressure and blood gases were measured in earlier studies and they were all within normal physiologic ranges during MRI measurements.[9,10] To avoid invasive catheterization of the femoral arteries, these measurements were not made in all subsequent studies. We are confident that these parameters were within normal ranges in these animals under these experimental preparations. This assertion is supported by our extensive experience on similar stroke studies, which arguably are more traumatic and yet these physiologic parameters under these experimental preparations were within normal ranges.

Hypercapnic Challenge

Hypercapnic challenges used a premixed gas of 5% CO_2 balanced with normal air. Each trial consisted of 4 minutes of baseline data acquisition, 3 minutes of data acquisition during hypercapnic challenge, and 3 minutes of data acquisition during the post-stimulation surveillance period.

MRI

Magnetic resonance imaging was performed on a rodent Bruker 7-Tesla BioSpec Scanner (Billerica, MA, USA) with 16-cm clear bore diameter. The animal was secured in a custom built, MRI compatible, rat head stereotaxic holder with ear and tooth bars.

Basal CBF (6 minutes) and hypercapnic challenge. Perfusion-weighted images were attained using the continuous arterial spin labeling[11] technique with single-shot, gradient-echo, echo-planar imaging (EPI) sequence with partial Flourier (5/8) acquisition. Continuous arterial spin labeling used a 2.7-seconds square radiofrequency pulse to the labeling coil. The other parameters were: seven 1.0-mm coronal images, field of view (FOV) = 2.56 × 2.56 cm, matrix 96 × 96 and reconstructed to 128 × 128, FOV = 2.56 × 2.56 cm, TR = 3 seconds (90° flip angle), and TE = 10.2 milliseconds. For basal CBF, 60 repetitions were obtained and averaged. For hypercapnic challenge, 100 repetitions were obtained.

Diffusion Tensor-weighted MRI (3.5 minutes). Diffusion tensor imaging were obtained with a single low *b*-value (10 s/mm^2) in 30 directions with a 1200 s/mm^2 b_{max}-value. EPI with partial Fourier (5/8) were also acquired using the following settings: seven 1.0-mm coronal images, FOV = 2.56 × 2.56 cm, matrix 96 × 96 and reconstructed to 128 × 128, single shot, TR = 3 seconds, TE = 32 milliseconds, $\Delta = 14$ milliseconds, $\delta = 5$ milliseconds, and two transients for signal averaging.[9,12,13]

T_2 map (9.5 minutes). T_2-weighted images were acquired using fast spin-echo sequence with TR = 3 seconds (90° flip angle), effective TE = 18, 54, 90, and 126 milliseconds, four echo train length. The other parameters were: seven 1.0-mm coronal images, FOV = 2.56 × 2.56 cm, matrix 96 × 96 and reconstructed to 128 × 128, and 8 transients for signal averaging.

Image Analysis

CBF, T_2, ADC, FA, and CO_2 reactivity maps were calculated as previously described.[9,12–14] Image maps of individual subjects were co-registered across time points via the application of a transformation matrix generated by QuickVol and MRIAnalysisPak software.[15] Three regions of interest (ROIs) were defined along the ipsilesional cortex, along with three ROIs in homologous regions of the contralesional hemisphere. The same ROIs were used to tabulate the CBF, T_2, ADC, FA, and CR values across all time points using Stimulate software (University of Minnesota). CBF, T_2, ADC, and FA of the ipsilesional ROI were normalized with respect to those of the contralesional ROI. Lesion volumes were defined by pixels that had T_2 values higher than the mean plus 2 s.d. of the value in the homologous contralesional region.

Histology

Immunohistology for glial fibrillary acidic protein (GFAP), neurons (NeuN), and microglia (Iba1) was assessed immediately after MRI experiments on day 14 post TBI. Briefly, selected rats were perfused 14 days post TBI with ice-cold 5% sucrose in heparinized phosphate-buffered saline, followed by ice-cold 4% buffered paraformaldehyde. Brains were removed and post-fixed for 2–5 hours at 4°C and subsequently cryopreserved in 30% sucrose for 2 days. Coronal sections (30-μm thick) were mounted on gelatin-coated slides and stored at −20 °C. Sections were processed using standard immunofluoresent staining against glial fibrilary acidic protein, NeuN and Iba-1 on separate serial sections correlating with MRI sections containing lesion. Briefly, sections were washed with phosphate-buffered saline followed by permeabilization using 0.2% Triton X-100 (2 μl Triton X-100:1 mL phosphate-buffered saline). The sections were blocked with 10% goat serum followed by incubation with a primary antibodies directed against GFAP (1:1,000 GenScript Rabbit Anti-GFAP pAb Cat# A01309), NeuN (1:200 Millipore Cat# MAB377), or Iba1 (1:500 abCam Cat# ab5076) diluted in goat serum overnight at 4 °C. The slides were then washed with phosphate-buffered saline and incubated with secondary antibody (GFAP secondary—1:200 dilution Alexa Fluoro 488 rabbit anti rat IgG; NeuN secondary—1:200 Alexa Fluoro 546 goat anti mouse IgG; or Iba1 secondary—1:500 Santa Cruz donkey anti-goat IgG-FITC) for 1 hour at 37 °C. Slides were washed and mounted with Vectashield containing DAPI (4',6-diamidino-2-phenylindole) (Vector Laboratories). Images were acquired on a Nikon C1si microscope (Melville, NY, USA) using × 10, × 20, and × 60 objectives.

Fluro Jade B Staining

Fluro Jade B is an anionic fluorescein derivative used to stain degenerating neurons.[16] Sections were incubated in a solution of 1%NaOH in 80% ethanol for 5 minutes followed by hydration in graded ethanols (75, 50, and 25%) to distilled water for 5 minutes each. The sections were then incubated for 10 minutes in 0.06% potassium permanganate, rinsed with distilled water and incubated in 0.004% Fluro Jade B (Hist-Chem, Jefferson, AR, USA) for 20 minutes. Sections were rinsed with distilled water three times for 2 minutes each. The slides were then dried on a slide warmer for 10 minutes, cleared with Histoclear and coverslipped with DPX (Fluka, Sigma-Aldrich, St Louis, MO, USA). Images were acquired on a Nikon C1si microscope using a × 20 and × 60 water immersion objective.

Functional Assessment

Sensorimotor function was assessed using the asymmetry forelimb placement (cylinder) test and foot-fault test.[8] Previous behavioral studies have demonstrated that these functional tests have the appropriate

sensitivity for this injury model.[17,18] Testing was conducted 1–3 days before TBI and again 1, 2, 7, and 14 days post TBI.

The forelimb asymmetry placement test was performed with videotaping to assess the use of forelimbs during exploration of the cylinder. The rat was placed in a transparent cylinder (20 cm diameter, 30 cm height) for 5 minutes or until 30 placements were made. A mirror was positioned under the cylinder to enable the video recorder to see directly into the cylinder. Behavior was scored by counting the number of left or right individual forelimb placements, and the number of simultaneous right and left[19] forelimb placements onto the wall of the cylinder during rearing. The forelimb asymmetry index was calculated as (the number of forelimb placements for each individual limb) +½ (number of both placements) divided by the total number of placements.

The forelimb foot-fault test was performed with videotaping to assess forelimb misplacement during locomotion. The rat was placed on an elevated grid floor (size 18 × 11 inches with grid openings of 1.56 × 1.00 inches) for 5 minutes or until 50 steps were taken with one (nonaffected) forelimb. The rat was allowed to move freely on the grid and the total number of steps and the number of times each limb fell below the grid opening were counted. The percentage of foot faults for each limb was calculated as the number of right or left forelimb foot faults divided by the total number of steps taken.

Statistical Analysis

Paired *t*-tests were used to compare CBF, CR, T_2, ADC, and FA abnormality between the ipsi- and contralesional sides. A one-way analysis of variance was also performed on each ROI analyzed to determine statistical significance amongst time points. A one-way analysis of variance was used to examine statistical significance between time points. Paired *t*-tests were used to compare asymmetry scores or foot-fault scores between pre-TBI and each subsequent time point. Values are presented as mean ± s.e.m. Statistical significance was set at $P < 0.05$.

RESULTS

Figure 1 shows representative CBF, T_2, ADC, FA, and CR maps from a single animal at 1 hour, 3 hours, 2, 7, and 14 days post TBI. At 1 and 3 hours, CBF MRI showed a substantial perfusion deficit in and around the impact area. The area of initial perfusion deficit was larger than the T_2, ADC, or FA abnormality at these time points. Within the area of impact (S1FL cortex), hyperperfusion was evident on day 2 followed by mild hypoperfusion on day 7 with a return toward normal values by day 14.

The T_2 abnormality (S1FL cortex) showed heterogeneous contrast across different time points, with hyperintensity indicating vasogenic edema and hypointensity indicating possible hemorrhage. The ADC maps in the S1FL cortex showed heterogeneous contrast, with hyperintensity indicating vasogenic edema and hypointensity indicating the presence of cytotoxic edema. The profiles of the T_2 and ADC abnormality appeared similar in temporal evolution peaking on day 2. They also appeared similar spatially, except in the superficial cortices. Hyperintensity in the corpus callosum was also observed on T_2 and ADC maps. FA decreases were also observed in the hyperacute phase, suggesting possible microstructural disruptions.

Cerebral blood flow percentage changes in response to CO_2 inhalation were negative at 1 and 3 hours in the ipsilesional cortex, in contrast to the positive response in the contralesional cortex. The area of negative response was markedly larger and showed larger negative% changes on day 2. CBF% changes in response to CO_2 returned toward positive, near-normal values by days 7 and 14.

CBF Values

Cerebral blood flow values were quantified using three ROIs along the ipsilesional and contralesional cortex for all time points. Cerebral blood flow in the contralesional ROIs did not change across all time points ($P > 0.05$, mean: 1.00 ± 0.15 mL/gram/min) and thus the CBF values in the ipsilesional hemisphere were normalized to the homologous regions in the contralesional hemisphere (Figure 2A). In the ipsilesional ROI 1, CBF was markedly reduced at 1 and 3 hours (10 and 20% of normal), markedly elevated on day 2 (2.5x of normal), slightly reduced on day 7, and returned toward near-normal values on day 14. In the ipsilesional ROI 2, CBF was significantly reduced at 1 and 3 hours (50% of normal), remained reduced on days 2 and 7 (but without hyperperfusion), and

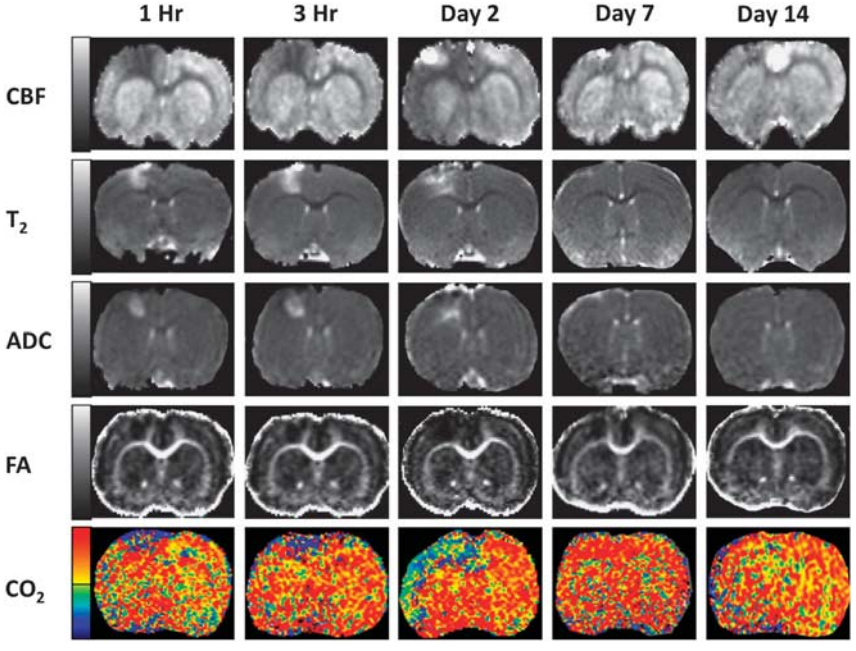

Figure 1. Representative cerebral blood flow, T_2, apparent diffusion coefficient, apparent diffusion coefficient, and CO_2 reactivity maps at 1 hour, 3 hours, and 2, 7, and 14 days post traumatic brain injury. Gray-scale Bar for cerebral blood flow: – 1 to 2.5 mL/g/min, T_2: 30 to 100 ms, apparent diffusion coefficient: 0.0004–0.0013 mm^2/s, fractional anisotropy: 0.1–0.6; color scale bar for CO_2 reactivity: – 100% (blue-purple) to 100% (red-yellow).

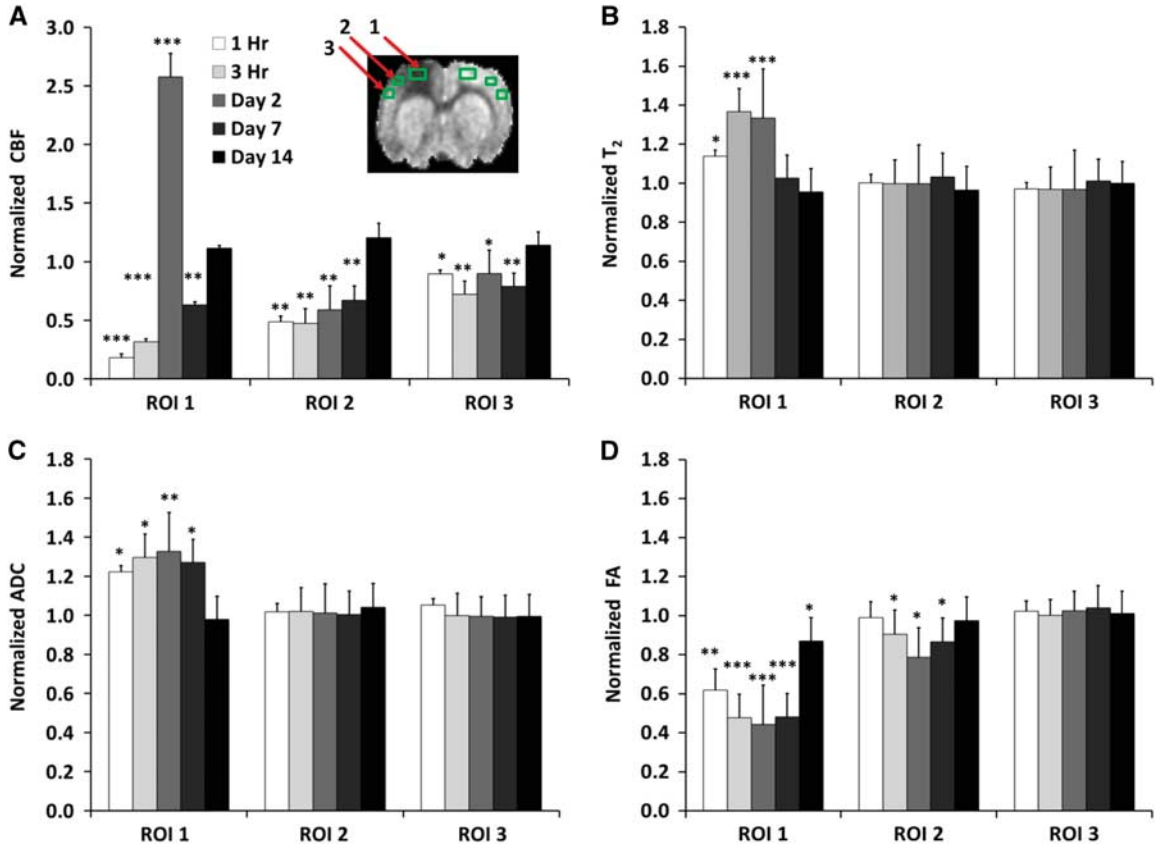

Figure 2. Normalized (**A**) cerebral blood flow, (**B**) T_2, (**C**) apparent diffusion coefficient, and (**D**) fractional anisotropy from the ipsilesional cortex at different time points after traumatic brain injury. Values were normalized to homologous region in the contralesional cortex (mean ± s.e.m., $n = 8$, * $P < 0.05$, ** $P < 0.01$, *** $P < 0.001$ between ipsilesional and contralesional sides). Cerebral blood flow, T_2, apparent diffusion coefficient, and fractional anisotropy of the homologous region in the contralesional cortex did not change with time and were not statistically different from sham-operated animals.

returned toward normal values on day 14. In the ipsilesional ROI 3, CBF was only slightly reduced at 1 and 3 hours, day 2, and day 7, and returned toward near-normal values on day 14.

T_2 Values

T_2 from the contralesional ROIs did not change across time ($P > 0.05$, mean: 55 ± 2ms). T_2 values of the ipsilesional ROIs were normalized to the contralesional ROIs (Figure 2B). In the ipsilesional ROI 1, T_2 was slightly elevated at 1 hour and further elevated at 3 hours, peaked on day 2, and returned toward (but did not reach) normal values on days 7 and 14. In the ipsilesional ROIs 2 and 3, by contrast, T_2 values did not change substantially across time.

ADC Values

Apparent diffusion coefficient in the contralesional ROIs did not change across time ($P > 0.05$, mean $0.70 \pm 0.02 \times 10^{-3}$ mm^2/s). All ADC values reported were normalized to the contralesional hemisphere (Figure 2C). In the ipsilesional ROI 1, ADC was elevated at 1 and 3 hours, peaked on day 2, and returned toward (but did not reach) normal values on day 14. In the contralesional and ipsilesional ROIs 2 and 3, ADC values were near-normal values at all time points studied.

FA Values

Fractional anisotropy in the contralesional ROIs did not change significantly across time ($P > 0.05$, mean: 0.23 ± 0.01). The normalized FA of the ipsilesional hemisphere are shown in Figure 2D. In the ipsilesional ROI 1, FA was markedly reduced at 1 hour and 3 hours, remained reduced on days 2 and 7 but returned toward normal values on day 14. In the ipsilesional ROI 2, FA values were near normal at 1 hour, slightly reduced at 3 hours, minimal on day 2 (suggesting delayed injury), and increased again by day 7, with a return toward near-normal values on day 14. In the ipsilesional ROI 3, T_2 MRI values were near-normal values at all time points studied.

Vascular Reactivity

In contrast to the parameters reported above, the CBF % changes in response to CO_2 were attenuated in the contralesional ROIs 1–3, and gradually recovered by day 14. In a separate group of sham-operated animals ($n = 3$), 5% CO_2 vascular CBF response was 79 ± 3%. In the ipsilesional ROI 1, CO_2 response was surprisingly negative at 1 and 3 hours, remained attenuated, yet positive on days 2 and 7, and returned toward near-normal values on day 14 (Figures 3A-3C).

Lesion Volumes

Figure 4 depicts the group-averaged temporal progression of lesion volumes defined by T_2 abnormality after TBI. T_2 lesion volumes were present at 1 hour, consistently peaked on day 2, and were markedly reduced by days 7 and 14.

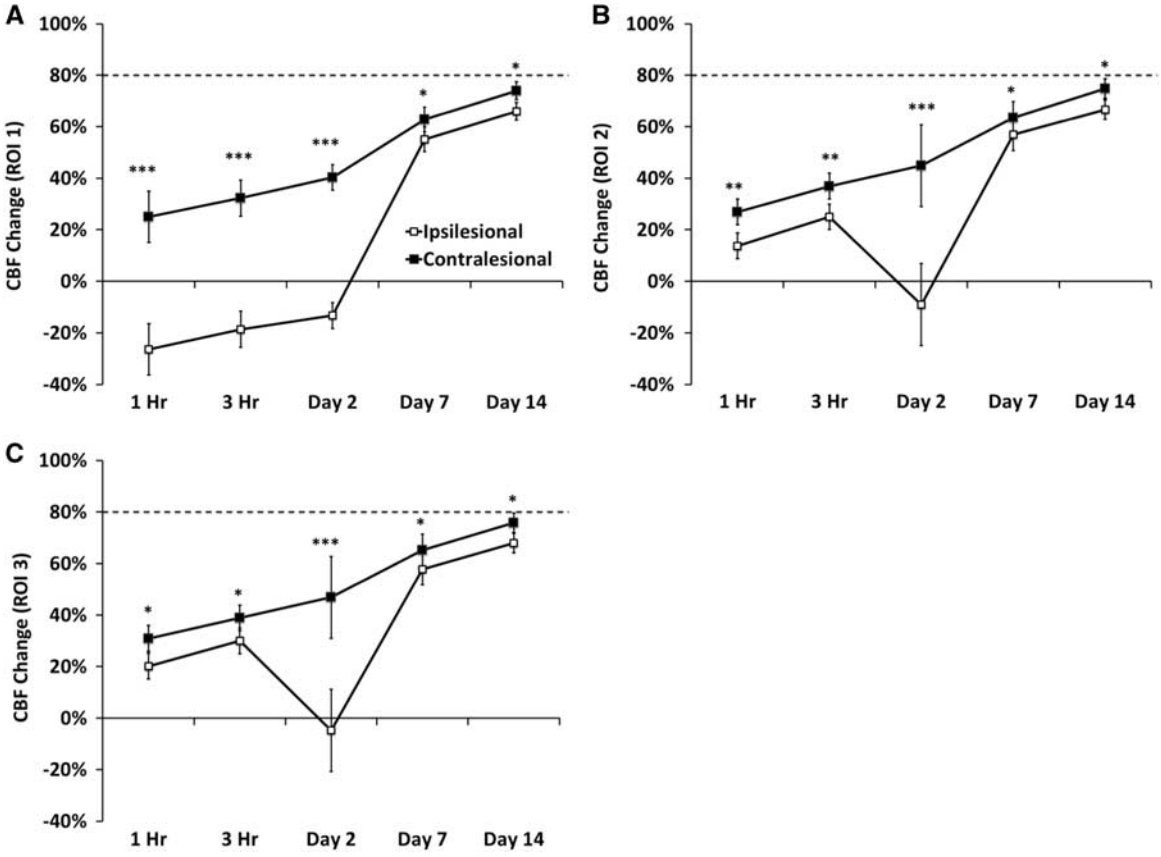

Figure 3. Line graphs of the temporal progression of % cerebral blood flow changes responding to 5% CO_2 challenge in the contralesional and ipsilesional cortices for (**A**) regions of interest 1, (**B**) regions of interest 2, and (**C**) regions of interest 3 (mean ± s.e.m., $n = 8$, * $P < 0.05$, ** $P < 0.01$, *** $P < 0.001$ between ipsilesional and contralesional sides).

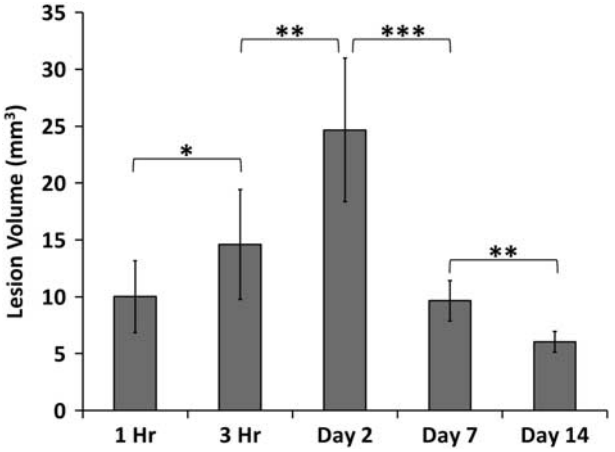

Figure 4. Bar graph of lesion volumes defined by T_2 abnormality at 1 hour, 3 hours, 2, 7, and 14 days post traumatic brain injury (mean ± s.e.m., $n = 8$, * $P < 0.05$, ** $P < 0.01$, *** $P < 0.001$). Lesion volumes were determined as pixels that had T_2 values higher than the mean plus 2 s.d. of the value in the homologous contralesional region.

Histology for GFAP, NeuN, and Iba1

Histologic assessment for expression of GFAP for reactive astrocytes, NeuN for neurons and DAPI for nuclei was performed 14 days post TBI in Sham and TBI animals in region 1 from Figure 2. Figure 5A shows representative images at ×20 and ×60 for DAPI (blue), GFAP (green), NeuN (red), and a composite image for each group. In sham animals there was little expression of GFAP, while in TBI animals there was a clear increase in the expression of GFAP suggesting the presence of reactive astrocytes in the area of impact (indicated by the gray arrows). Neurons were detected using an antibody directed against NeuN. Neuronal soma morphology was normal in sham animals while in TBI animals we detected punctate and abnormal morphologic changes (shown by white arrows) under the area of impact suggesting neuronal damage.

Histologic assessment for expression of Iba1 for microglia and DAPI for nuclei was performed 14 days post TBI in Sham and TBI animals in region 1 from Figure 2. Figure 5B shows representative images at ×10 and ×20 for DAPI (blue) and Iba1 (green) and a composite image for each group. In Sham animals there was little detection of Iba1 positive cells, while in TBI animals there was increased microglial infiltration in the area surrounding the impact.

Fluro Jade B staining

Fluro Jade B staining for degenerating neurons was performed 14 days after TBI in sham or TBI animals in region 1 from Figure 2. Figure 6A demonstrates representative images from the cortex from sham and TBI animals. In the Sham group, the number of Fluro Jade B positive cells (white arrows) in the ipsilesional S1 cortex was 20.52 ± 1.95 cells per field ($N = 6$, $P < 0.05$; Figure 6B). In the TBI group, the number of Fluro Jade B positive cells in the ipsilesional S1 cortex was 73.8 ± 4.24 cells per field ($N = 6$,

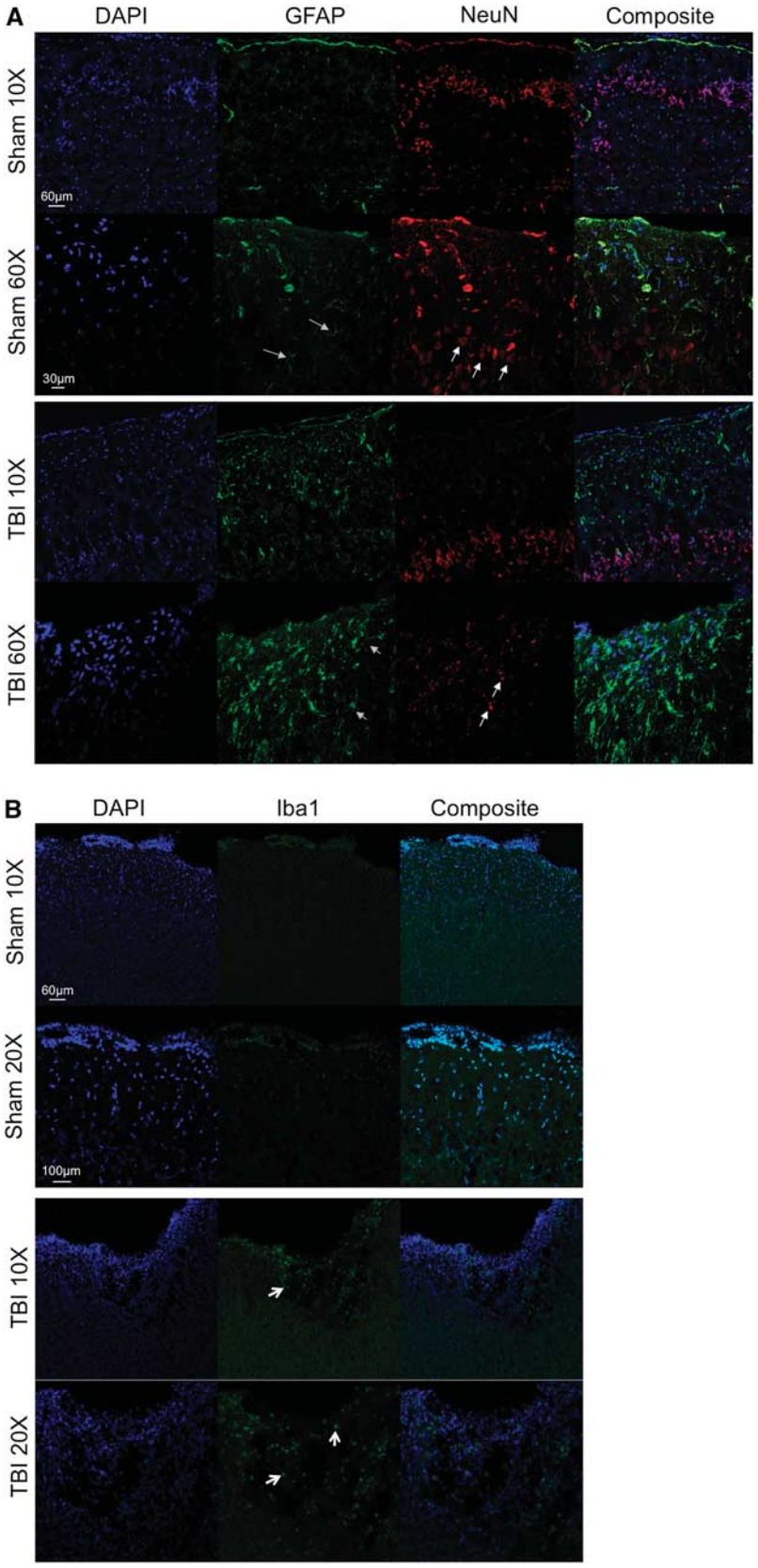

Figure 5. (**A**) Representative images for both Sham and traumatic brain injury animals are shown at ×20 and ×60 for DAPI (blue), glial fibrillary acidic protein (green), neurons (red) and a composite image. White arrows indicate normal neuronal soma morphology in Sham animals and abnormal morphology in traumatic brain injury animals. Gray arrows indicate glial fibrillary acidic protein positive cells in both Sham and traumatic brain injured animals. (**B**) Representative images for Sham and traumatic brain injury animals are shown at ×10 and ×20 for DAPI (blue) and Iba1 (green) and a composite image for each group. White arrows indicate Iba1 positive cells in the traumatic brain injury animals.

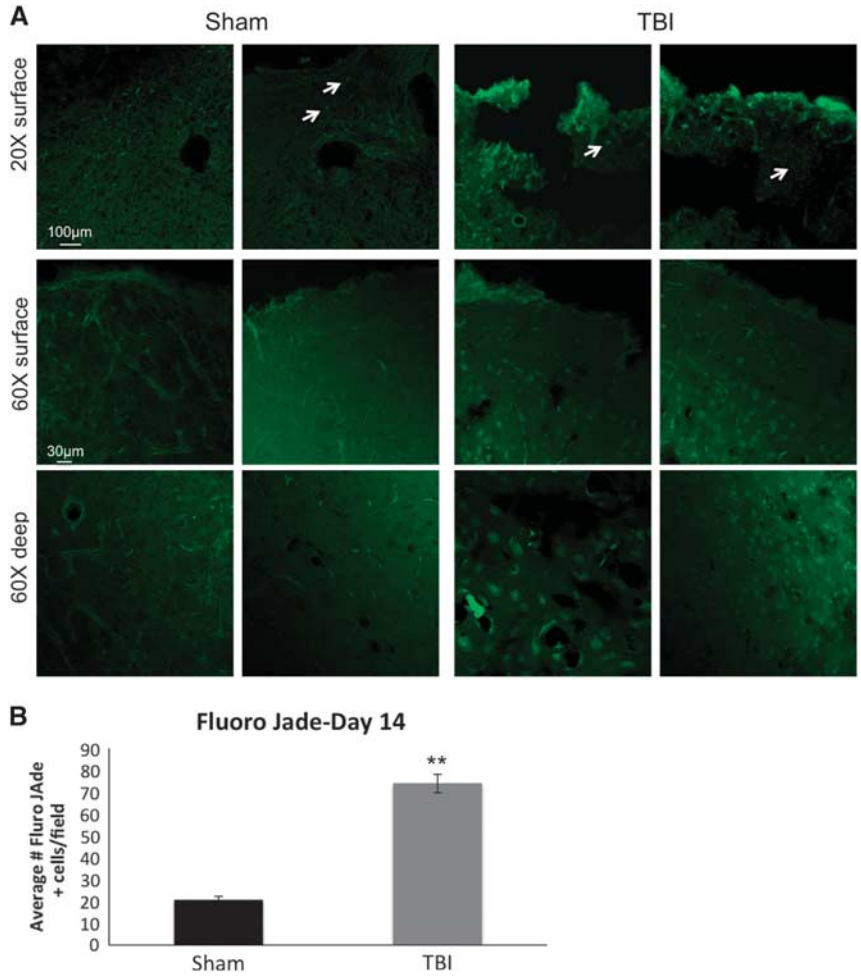

Figure 6. (**A**) Representative images for Fluro Jade staining (green) are shown at × 20 and × 60 from the cortex of sham and traumatic brain injury animals. Positive Fluro Jade cells are indicated by white arrows. (**B**) Histogram demonstrating the average number of Fluro Jade positive cells within the cortex in sham and traumatic brain injury animals on day 14 post traumatic brain injury.

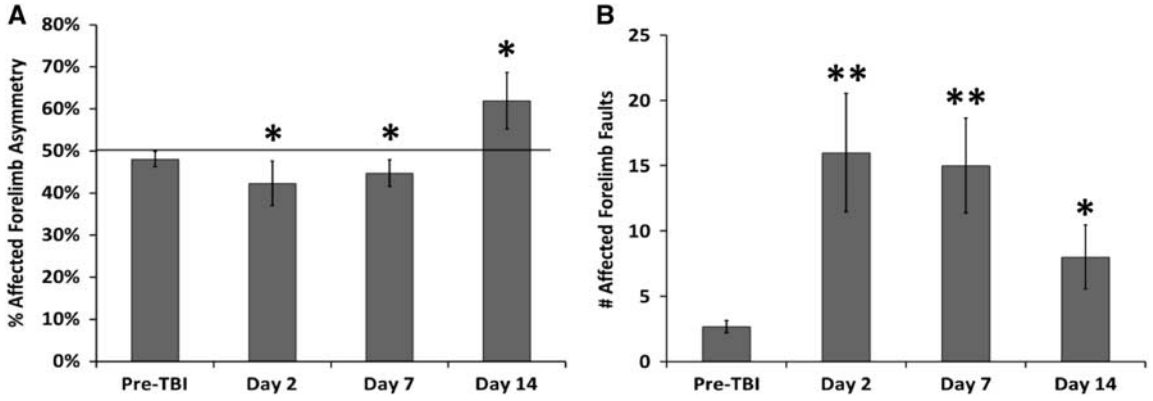

Figure 7. Bar graphs of the (**A**) affected forelimb asymmetry and (**B**) affected forelimb fault scores at pre-traumatic brain injury, 2, 7, and 14 days post traumatic brain injury (mean ± s.e.m., $n = 8$, * $P < 0.05$, ** $P < 0.01$ between scores of Pre-traumatic brain injury and each subsequent time point).

$P < 0.05$) (Figure 6B). The numbers of Fluro Jade B positive cells in the ipsilesional S1 cortex were significantly different between the Sham and TBI groups ($P < 0.05$). The results from the Fluro Jade B experiments demonstrate increased neurodegeneration after TBI.

Behavioral Outcomes

The mean scores for the forelimb placement asymmetry and the foot-fault tests are shown in Figures 7A and 7B, respectively. Pre-TBI affected forelimb asymmetry was 47 ± 3%, indicating mostly

symmetrical use of both forelimbs. The asymmetry score was the worst on day 2 post TBI (41 ± 4%, respectively), indicating decreased utilization of the affected forelimb (right). Pre-TBI foot-fault scores were 3.53 ± 0.42%. After TBI, foot-fault scores were the worst in the affected forelimb (right) on day 2 (16.4 ± 4.8%), improved slightly on day 7 (14.9 ± 3.1%), and returned toward the pre-TBI value on day 14 post TBI (9.5 ± 2.5%).

Sham Group

In sham-operated animals ($n = 3$) T_2, ADC, FA, and basal CBF were not statistically different between the two hemispheres, did not change across time up to 14 days, and were not statistically different from those in the contralesional hemisphere of the TBI group. Additionally, sham-operated animals CBF fMRI response to 5% CO_2 was 79 ± 3%, and was not statistically different between the two hemispheres.

DISCUSSION

This study characterized the effects of perturbed CBF and CR on T_2, ADC, FA and behavioral scores in an open-skull, CCI TBI model in rats. In addition, we assessed changes in GFAP, NeuN, Iba1, and Fluro Jade staining in Sham and TBI animals. The major findings were: (i) in the contralesional cortex, the CBF, T_2 ADC, and FA were not affected at all time points studied, but the CR was reduced followed by a gradual recovery from days 0 to 14; (ii) in the ipsilesional cortex, the abnormal areas of the CBF and CR on days 0 and 2 were larger than those of the T_2, ADC, and FA which were localized to the area of impact; (iii) within the area of impact, CBF was reduced on day 0, increased to 2.5 times of normal on day 2, and returned toward normal by day 14, whereas in the tissue surrounding the impact, hypoperfusion was observed only on days 0 and 2; (iv) CBF response in the ipsilesional hemisphere was negative in the ipsilesional cortex, most severe on day 2 but gradually returned toward normal; (v) T_2, ADC, and FA abnormalities in the impact core were observed on day 0, peaked on day 2, and gradually returned towards normal by day 14, whereas these parameters in the tissue surrounding the core were only mildly affected; (vi) lesion volumes, peaked on day 2 and were temporally correlated with behavioral scores; (vii) it appears that T_2, ADC, and FA abnormality only occurred in areas where blood flow was perturbed to the point of being ischemic (~ ⩽30% of normal); (viii) CBF and CR were significantly disrupted in the tissue surrounding the impact site in a time-dependent manner but most tissue eventually recovered; (ix) on day 14 there was increased expression of both reactive astrocytes and microglia surrounding the area of impact, and; and (x) there was increased neurodegeneration detected by Fluro Jade and by NeuN staining in TBI animals compared with Sham.

Cortical Blood Flow

In the contralesional cortex, CBF was not affected by TBI across all time points. In the ipsilesional cortex immediately below the impact area (ROI 1), we observed hypoperfusion at 1–3 hours and hyperperfusion on day 2 indicating that there were marked hemodynamic disturbance after TBI. Hyperperfusion on day 2 coincided with the peak of T_2 hyperintensity (vasogenic edema). In the tissue surrounding the impact core (ROIs 2 and 3), CBF was mildly reduced 1–3 hours after TBI, further reduced on day 2 and gradually recovered toward normal by day 14 (but no hyperperfusion). The reduced CBF is likely due to local increases in intracranial pressure and/or damaged to blood vessels.

CBF disturbances have been reported in the literature ranging from studies reporting only hypoperfusion after TBI, while others have observed both hypoperfusion and hyperperfusion after TBI. Thomale *et al.*[20] found severe hypoperfusion (by laser Doppler flowmetry) in the area of the impact at 0.5–6.0 hours and hyperperfusion at 24 and 48 hours in a similar rat model of moderate CCI. Immonen *et al.*[21] found that cerebral blood volume dropped 1 hours after injury, pseudonormalized on days 1–3 and increased on day 4 in a similar CCI model. Other studies found CBF reduction on day 0 using the Marmarou rat model[6] or fluid percussion model[22] but without hyperperfusion on subsequent days after TBI. The differences in CBF disruptions amongst different studies are likely because of differences in TBI model and severity of injury. The novelty of our work is that it used relatively high spatial resolution, quantitative CBF MRI techniques which afforded longitudinal measurements. Moreover, we analyzed data to determine the effects of perturbed CBF had on T_2, ADC, and FA within and surrounding the impact area, providing valuable insights into tissue fate.

The mechanisms underlying hypoperfusion could be due to physical damage to the vessels or increased intracranial pressure. The mechanisms underlying hyperperfusion could arise from accumulated by-products (such as free radicals) and vasoactive metabolites (such as lactic acid and adenosine) that could induce vasodilation through relaxation of vascular smooth muscle.[23,24] Some of these metabolites are implicated in modulating blood–brain-barrier permeability,[25] which could potentially enhance cerebral edema. Others have suggested neurogenic vasodilation[26] and passive physiologic coupling.[27] Our findings herein suggest that hyperperfusion on day 2 coincided with the peak of T_2 hyperintensity (vasogenic edema) and was not beneficial although the tissue was able to recover substantially by day 14, in marked contrast to the outcome found in ischemic stroke.[28]

Cerebrovascular Reactivity

In sham-operated animals, CBF fMRI response to 5% CO_2 was 79 ± 3%, consistent with previous reports in normal animals under essentially identical experimental conditions.[13,29] In the contralesional cortex of TBI animals, vascular reactivity was significantly reduced on days 0 and 2, and gradually returned toward normal by days 7 and 14, in marked contrast to T_2, ADC, FA, and basal CBF in the contralesional cortex, which was not significantly affected by TBI. These findings suggest that a systemic cardiovascular disturbance that affects global CBF responses to hypercapnia could make other brain regions more susceptible to hypoxic injury.

In the ipsilesional cortex, negative CBF responses to hypercapnia were observed in the area of impact, and such negative CBF responses were found to be the worst on day 2 but slowly returned toward positive and normal values by day 14. The tissue surrounding the impact core also showed reduced or negative CBF responses on day 0. The extent of the area and magnitude of negative CBF responses were most dramatic on day 2, affecting a large portion of the cortex. The negative CBF response to hypercapnia, a novel finding in TBI, was likely attributed to a blood-stealing phenomenon, in which vessels in surrounding normal tissue vasodilated in response to CO_2, whereas vessels in the injured tissue could not. Such a blood-stealing phenomenon has been observed in ischemic stroke, and ischemic cerebrovascular disease.[30–32]

Attenuated CBF responses to vasodilation have been reported using both the CCI[33,34] and fluid percussion injury models.[35] However, negative CBF responses to hypercapnia have not been reported previously. The differences in CR disruption amongst different studies could be due to differences in TBI model and severity of injury, as well as possible differences in anesthetics used.

The Impact of Hemodynamic Disturbances on Cortical T_2, ADC, and FA

Although a few studies have reported hemodynamic disturbances in TBI, the effects of CR, hypo- and hyperperfusion on T_2, ADC, and FA have not been systematically studied. We found that the area

of perfusion deficit and CR was generally larger than the T_2, ADC, or FA abnormality on days 0 and 2, while T_2, ADC, and FA abnormality were isolated to the area of impact. The patterns of T_2, ADC, and FA changes after TBI are in general agreement with those reported from our previous studies[8,36] and other studies.[37–39]

In the impacted region (R0I-1), average CBF reached ischemic levels (⩽20% of normal) at 1 and 3 hours, which is expected to cause ischemia and to manifest in detectable T_2 and ADC changes as observed. Interestingly, at 14 days there were no apparent large infarcts detected based on MRI and behavioral scores indicating that outcome measures were returning toward normal, consistent with our previous study.[36] However, histologic analysis 14 days post TBI of Fluro Jade, which detects neurodegenerating neurons, in conjunction with NeuN staining revealed substantial neuronal cell death in the tissue surrounding the impact zone. Furthermore, we detected substantial infiltration of microglia, the immune cells of the brain, and increased expression of GFAP, which indicates the presence of reactive astrocytes. These data suggest that even when MRI appears normal there are still substantial changes that can be detected at the cellular level. Previous histologic studies showed that there was only some detectable cell death in the same animal model,[8,36] suggesting that most tissue showed normalized T_2 and ADC. It is likely that there was substantial recovery along with some functional compensation.

In tissue surrounding the impact (ROI 2), CBF dropped by 50%; however, no T_2 or ADC abnormalities were observed, except a mild reduction in FA. In ROI 3, CBF dropped by ~20%, with no T_2, ADC, or FA abnormalities observed. Nonetheless, it is possible that mild hypoperfusion for a few days could have negative consequences on cellular physiology, resulting in disruption of cellular function long term (beyond 14 days).

In sum, hemodynamic disturbances in TBI have direct effects on T_2, ADC, and FA. However, T_2, ADC, and FA may not be sufficiently sensitive to detect subtle changes of cell injury and cell death during the chronic phase. Developing new or improving the sensitivity of current imaging biomarkers for the chronic TBI phase is needed. Nonetheless, CBF MRI has the potential to provide additional and unique insights into TBI that complement other MRI techniques.

The Impact of Hemodynamic Disturbances on Behavioral Outcomes

The temporal profiles of neurologic function after TBI are consistent with those reported previously in the same CCI model.[8,36] Changes in CBF and CR have significant effects on anatomic MRI and thus it is not surprising that CBF and CR are correlated with behavioral scores in general. Recovery of function requires normalization of CBF and CR. It is however worth-mentioning that we found differences between the forelimb symmetry and foot-fault scores. Affected forelimb fault scores were still considerably worse than pre-TBI values on day 7 but returned closer to normal values on day 14. This is in marked contrast to affected forelimb asymmetry scores. The differences between the two behavioral tests suggest that the affected forelimb fault test is more sensitive to mild TBI than the asymmetry test. Fundamentally the two tests measure similar deficits in sensorimotor function. However, the foot-fault test requires proper limb placement and sensory feedback, whereas the asymmetry test assesses the rodent's voluntary use of the forelimbs during upright exploration.[17] Both behavioral tests provided different, but complementary, information about TBI injury. Future studies will used more sensitive tests such as the Vermicelli handling test or the beam walk test.

Comparison with Stroke

The spatiotemporal characteristics of CBF, CR, T_2, ADC, and FA changes showed some similarities and differences when compared with those of ischemic stroke. In both TBI and ischemic stroke, heterogeneous hypoperfusion is apparent immediately after injury and the areas of hypoperfusion are generally larger than ADC and T_2 changes. Hyperperfusion is often observed 1–2 days after injury. The outcome of tissue exhibiting hyperperfusion in ischemic stroke is usually infarction[28] whereas in this TBI model, there was substantial recovery. After both ischemic stroke[28] and TBI, negative CR has been observed on the ipsilesional side indicating possible autoregulatory dysfunction. In ischemic stroke, CR in the contralesional cortex was mostly normal whereas in our model of TBI, CR was attenuated.

In ischemic stroke, ADC decreases are apparent within a few minutes, whereas T_2 increases are not apparent for several hours to a day after stroke in rats. T_2 hyperintensity in ischemic stroke also usually indicates irreversible injury.[14,40] In our TBI model, T_2 increases were apparent by 1 hour post TBI, peaked on day 2 and mostly returned toward normal by day 14, suggesting that the initial presence of vasogenic edema after TBI is mostly reversible. These differences in CBF, CR, T_2, ADC, and FA characteristics offer important insights into the differences in pathophysiologic changes occurring in TBI and stroke.

CONCLUSIONS

This study presented a systematic characterization of quantitative multi-parametric MRI of the spatiotemporal changes in an open-skull, CCI TBI model in rats. We found significant hemodynamic disturbances in cerebral blood flow and cerebrovascular reactivity after TBI and they exerted observable effects on lesion volume, T2 and diffusion parameters. Future studies will investigate impacts to different brain regions (i.e., the hippocampus) and repeated closed skull TBI, improve MRI sensitivity to more subtle injury, and incorporate blood volume MRI, resting-state fMRI, and additional behavioral measures (i.e., memory function) to further characterize TBI.

AUTHOR CONTRIBUTIONS

JAL, LTW, and TD designed the study; JAL, LTW, WL, QS, EM, SH, and TD developed the methodology; JAL, LTW, RCB, and AS collected the data; JAL, LTW, RCB, and AS performed the analysis; and JAL, LTW, and TD wrote the manuscript.

DISCLOSURE/CONFLICT OF INTEREST

The authors declare no conflict of interest.

ACKNOWLEDGMENTS

We thank Timothy Schallert and Theresa Jones of UT Austin for their assistance in the setup of the behavioral assays used in this study.

REFERENCES

1 Coronado VG, McGuire LC, Sarmiento K, Bell J, Lionbarger MR, Jones CD *et al.* Trends in Traumatic Brain Injury in the U.S. and the public health response: 1995-2009. *J Safety Res* 2012; **43**: 299–307.
2 McIntosh TK, Vink R, Noble L, Yamakami I, Fernyak S, Soares H *et al.* Traumatic brain injury in the rat: characterization of a lateral fluid-percussion model. *Neuroscience* 1989; **28**: 233–244.
3 Feuerstein D, Takagaki M, Gramer M, Manning A, Endepols H, Vollmar S *et al.* Detecting tissue deterioration after brain injury: regional blood flow level versus capacity to raise blood flow. *J Cereb Blood Flow Metab* 2014; **34**: 1117–1127.
4 Thomale UW, Kroppenstedt SN, Beyer TF, Schaser KD, Unterberg AW, Stover JF. Temporal profile of cortical perfusion and microcirculation after controlled cortical impact injury in rats. *J Neurotrauma* 2002; **19**: 403–413.

5 Pasco A, Lemaire L, Franconi F, Lefur Y, Noury F, Saint-Andre JP *et al.* Perfusional deficit and the dynamics of cerebral edemas in experimental traumatic brain injury using perfusion and diffusion-weighted magnetic resonance imaging. *J Neurotrauma* 2007; **24**: 1321–1330.
6 Shen Y, Kou Z, Kreipke CW, Petrov T, Hu J, Haacke EM. *In vivo* measurement of tissue damage, oxygen saturation changes and blood flow changes after experimental traumatic brain injury in rats using susceptibility weighted imaging. *Magn Reson Imaging* 2007; **25**: 219–227.
7 Hayward NM, Tuunanen PI, Immonen R, Ndode-Ekane XE, Pitkanen A, Grohn O. Magnetic resonance imaging of regional hemodynamic and cerebrovascular recovery after lateral fluid-percussion brain injury in rats. *J Cereb Blood Flow Metab* 2011; **31**: 166–177.
8 Watts LT, Long J, Chemello J, Van Koughnet S, Fernandez A, Huang S *et al.* Methylene Blue is Neuroprotective against mild traumatic brain injury. *J Neurotrauma* 2014; **31**: 1063–1071.
9 Sicard KM, Duong TQ. Effects of hypoxia, hyperoxia and hypercapnia on baseline and stimulus-evoked BOLD, CBF and CMRO2 in spontaneously breathing animals. *NeuroImage* 2005; **25**: 850–858.
10 Duong TQ, Iadecola C, Kim SG. Effect of hyperoxia, hypercapnia, and hypoxia on cerebral interstitial oxygen tension and cerebral blood flow. *Magn Reson Med* 2001; **45**: 61–70.
11 McCasland JS, Woolsey TA. High-resolution 2-deoxyglucose mapping of functional cortical columns in mouse barrel cortex. *J Comp Neurology* 1988; **278**: 555–569.
12 Shen Q, Ren H, Cheng H, Fisher M, Duong TQ. Functional, perfusion and diffusion MRI of acute focal ischemic brain injury. *J Cereb Blood Flow and Metab* 2005; **25**: 1265–1279.
13 Sicard K, Shen Q, Brevard ME, Sullivan R, Ferris CF, King JA *et al.* Regional cerebral blood flow and BOLD responses in conscious and anesthetized rats under basal and hypercapnic conditions: implications for functional MRI studies. *J Cereb Blood Flow Metab* 2003; **23**: 472–481.
14 Shen Q, Meng X, Fisher M, Sotak CH, Duong TQ. Pixel-by-pixel spatiotemporal progression of focal ischemia derived using quantitative perfusion and diffusion imaging. *J Cereb Blood Flow and Metab* 2003; **23**: 1479–1488.
15 Liu ZM, Schmidt KF, Sicard KM, Duong TQ. Imaging oxygen consumption in forepaw somatosensory stimulation in rats under isoflurane anesthesia. *Magn Reson Med* 2004; **52**: 277–285.
16 Schmued LC, Hopkins KJ. Fluoro-Jade: novel fluorochromes for detecting toxicant-induced neuronal degeneration. *Toxicol Pathol* 2000; **28**: 91–99.
17 Baskin YK, Dietrich WD, Green EJ. Two effective behavioral tasks for evaluating sensorimotor dysfunction following traumatic brain injury in mice. *J Neurosci Methods* 2003; **129**: 87–93.
18 Soblosky JS, Matthews MA, Davidson JF, Tabor SL, Carey ME. Traumatic brain injury of the forelimb and hindlimb sensorimotor areas in the rat: physiological, histological and behavioral correlates. *Behav Brain Res* 1996; **79**: 79–92.
19 WP J, CB F, GB R. Metabolic engineering of sugars and simple sugar derivatives in plants. *Plant Biotechnol J* 2013; **11**: 142–156.
20 Thomale UW, Schaser K, Kroppenstedt SN, Unterberg AW, Stover JF. Cortical hypoperfusion precedes hyperperfusion following controlled cortical impact injury. *Acta Neurochir Suppl* 2002; **81**: 229–231.
21 Immonen R, Heikkinen T, Tahtivaara L, Nurmi A, Stenius TK, Puolivali J *et al.* Cerebral blood volume alterations in the perilesional areas in the rat brain after traumatic brain injury—comparison with behavioral outcome. *J Cereb Blood Flow Metab* 2010; **30**: 1318–1328.
22 Pasco A, Lemaire L, Franconi F, Lefur Y, Noury F, Saint-Andre JP *et al.* Perfusional deficit and the dynamics of cerebral edemas in experimental traumatic brain injury using perfusion and diffusion-weighted magnetic resonance imaging. *J Neurotrauma* 2007; **24**: 1321–1330.
23 Kontos HA, Wei EP. Oxygen-dependent mechanisms in cerebral autoregulation. *Ann Biomed Eng* 1985; **13**: 329–334.
24 Berne RM, Rubio R. Regulation of coronary blood flow. *Adv Cardiol* 1974; **12**: 303–317.
25 Joo F. The blood-brain barrier. New aspects to the function of the cerebral endothelium. *Nature* 1986; **321**: 197–198.
26 Macfarlane R, Moskowitz MA, Sakas DE, Tasdemiroglu E, Wei EP, Kontos HA. The role of neuroeffector mechanisms in cerebral hyperperfusion syndromes. *J Neurosurg* 1991; **75**: 845–855.
27 Marchal G, Furlan M, Beaudouin V, Rioux P, Hauttement JL, Serrati C *et al.* Early spontaneous hyperperfusion after stroke. A marker of favourable tissue outcome? *Brain* 1996; **119**: 409–419.
28 Shen Q, Du F, Huang S, Duong TQ. Spatiotemporal characteristics of postischemic hyperperfusion with respect to changes in T1, T2, diffusion, angiography, and blood–brain barrier permeability. *J Cereb Blood Flow Metab* 2011; **31**: 2076–2085.
29 Lee JG, Hudetz AG, Smith JJ, Hillard CJ, Bosnjak ZJ, Kampine JP. The effects of halothane and isoflurane on cerebrocortical microcirculation and autoregulation as assessed by laser-Doppler flowmetry. *Anesth Analg* 1994; **79**: 58–65.
30 Paksoy Y, Genc BO, Genc E. Retrograde flow in the left inferior petrosal sinus and blood steal of the cavernous sinus associated with central vein stenosis: MR angiographic findings. *AJNR Am J Neuroradiol* 2003; **24**: 1364–1368.
31 Poublanc J, Han JS, Mandell DM, Conklin J, Stainsby JA, Fisher JA *et al.* Vascular steal explains early paradoxical blood oxygen level-dependent cerebrovascular response in brain regions with delayed arterial transit times. *Cerebrovasc Dis Extra* 2013; **3**: 55–64.
32 Arteaga DF, Strother MK, Faraco CC, Jordan LC, Ladner TR, Dethrage LM *et al.* The vascular steal phenomenon is an incomplete contributor to negative cerebrovascular reactivity in patients with symptomatic intracranial stenosis. *J Cereb Blood Flow Metab* 2014; **34**: 1453–1462.
33 Golding EM, Steenberg ML, Contant CF, Jr., Krishnappa I, Robertson CS, Bryan RM, Jr. Cerebrovascular reactivity to CO(2) and hypotension after mild cortical impact injury. *Am J Physiol* 1999; **277**: H1457–H1466.
34 Forbes ML, Hendrich KS, Kochanek PM, Williams DS, Schiding JK, Wisniewski SR *et al.* Assessment of cerebral blood flow and CO2 reactivity after controlled cortical impact by perfusion magnetic resonance imaging using arterial spin-labeling in rats. *J Cereb Blood Flow Metab* 1997; **17**: 865–874.
35 Lewelt W, Jenkins LW, Miller JD. Effects of experimental fluid-percussion injury of the brain on cerebrovascular reactivity of hypoxia and to hypercapnia. *J Neurosurg* 1982; **56**: 332–338.
36 Long JA, Watts LT, Chemello J, Huang S, Shen Q, Duong TQ. Multiparametric and longitudinal MRI characterization of mild traumatic brain injury in rats. *J Neurotrauma* 2014; **32**: 598–607.
37 Immonen RJ, Kharatishvili I, Grohn H, Pitkanen A, Grohn OH. Quantitative MRI predicts long-term structural and functional outcome after experimental traumatic brain injury. *NeuroImage* 2009; **45**: 1–9.
38 Lescot T, Fulla-Oller L, Po C, Chen XR, Puybasset L, Gillet B *et al.* Temporal and regional changes after focal traumatic brain injury. *J Neurotrauma* 2010; **27**: 85–94.
39 Xu S, Zhuo J, Racz J, Shi D, Roys S, Fiskum G *et al.* Early microstructural and metabolic changes following controlled cortical impact injury in rat: a magnetic resonance imaging and spectroscopy study. *J Neurotrauma* 2011; **28**: 2091–2102.
40 Shen Q, Fisher M, Sotak CH, Duong TQ. Effects of reperfusion on ADC and CBF pixel-by-pixel dynamics in stroke: characterizing tissue fates using quantitative diffusion and perfusion imaging. *J Cereb Blood Flow Metab* 2004; **24**: 280–290.